



# Role of the preferential flow at rock–soil interface in the water leaking process in near-surface fissures filled with soils in the karst rock desertification area

Tingting Liu<sup>1,2</sup> · Xudong Peng<sup>1,2</sup> · Quanhou Dai<sup>1,2,3</sup> · Shengbing Xu<sup>1,2</sup>

Received: 9 March 2022 / Accepted: 28 June 2022 / Published online: 2 August 2022  
© The Author(s) 2022

## Abstract

Soil preferential flow infiltrating rapidly through the rock–soil interface is an important hydrological process in karst rocky desertification area. However, how does the water leakage in the near-surface fissures, especially those filled with soil, proceed? The role of preferential flow at rock–soil interface of those fissures on water leakage process still puzzles us. The goal of this study was to reveal the role of soil preferential flow at the rock–soil interface in the process of water leaking of near-surface fissures. Five typical types of near-surface fissures were selected in an area experiencing severe rocky desertification in Guizhou Province, China. Dye tracer testing was applied, combined with digital image processing techniques. The results indicated that the rock–soil interface flow on both sides of the fissures is the most important preferential flow form in the fissures in karst area. The dyed area ratio of preferential flow varied from 0.12 to 0.48 in the rock + soil profiles, from 0.06 to 0.37 in the soil profiles, and between 0.02 and 0.16 in the rock–soil interface. The rock–soil interface is the smallest in terms of both their variation range of dyed area ratio and preferential flow patterns compared with soil and rock–soil profiles. The soil preferential flow in near-surface fissures mainly occurs in the soil depth range of 0–20 cm. The preferential flow path is mainly affected by the rock–soil interface on both sides and can pass through the clay layer with poor permeability. However, the soil depth of the dyed part was more than 50 cm. The soil preferential flow at the rock–soil interface is the main form of rapid downward leakage of water in near-surface fissures in the karst rocky desertification area, which can flow to the bottom of clay layer with poor permeability.

**Keywords** Rock–soil interface · Preferential flow · Dye tracing · Rocky desertification

## Introduction

At present, karstic areas around the world cover approximately 22 million km<sup>2</sup>, accounting for 12% of the total land area of the world (Liu et al. 2020). The karstic area of China covers approximately 3.44 million km<sup>2</sup>, accounting for 1/3

of the total land area (Song et al. 2017), among which that in Southwest China totals approximately 0.54 million km<sup>2</sup>. This area is well known as the largest karst ecosystem in the world. As a famous karst province, most of Guizhou Province belongs to the karst area (Zhang et al. 2001). Rock desertification, as the most serious environmental problem affecting karst areas, forms when rocks are gradually exposed to the surface due to soil erosion or leakage loss. Under the joint actions of karstic and anthropogenic activities, carbonate rocks develop into karst grooves and near-surface fissures (White 1995). In fact, Guizhou Province has a subtropical monsoon climate. There is plenty of precipitation feeding the rocky desertification area with rainfall averages approximately 1100–1300 mm yr<sup>-1</sup>. However, this area has dual space structures of surface and underground, with thin soil cover, low total amount of soil, low water storage capacity and developed fissures. The downward leakage of water is an important process that causes soil underground

✉ Xudong Peng  
bjpxd@126.com; xdpeng@gzu.edu.cn

<sup>1</sup> College of Forestry, Guizhou University, Guiyang 550025, People's Republic of China  
<sup>2</sup> Institute of Soil Erosion and Ecological Restoration, Guizhou University, Guiyang 550025, People's Republic of China  
<sup>3</sup> The Key Laboratory of Plant Resource Conservation and Germplasm Innovation in Mountainous Region (Ministry of Education), Collaborative Innovation Center for Mountain Ecology and Agro-Bioengineering (CICMEAB), Guizhou University, Guiyang 550025, People's Republic of China

leakage and further aggravates rocky desertification-derived drought (Wang et al. 2014; Oberle et al. 2016). Therefore, it is of great significance to study the process and characteristics of water leakage in karstic rocky desertification areas.

Because of its special dual hydrogeological structure in the karst rocky desertification area (Li et al. 2016), the soil cover on the surface is thin and discontinuous with weak water-holding capability (Wang et al. 2014). Rainfall can easily infiltrate into underground systems through soil, as well as fissures and conduits. Groundwater is abundant but short of surface water, which makes it difficult for rainwater to be used by plants and leads to drought of rocky desertification (Chen et al. 2013). In addition, the exposed rate of bedrock in the severely rocky desertification area is high, and the rock-soil interface is widely distributed. It increases the complexity and heterogeneity of water movement in this area (White 2002). It is very difficult to directly monitor the downward leakage of water in karst areas. How to observe the process of water downward leakage intuitively becomes a technical problem that needs to be solved in this field. Water infiltration is an important link and process for the mutual transformation of surface runoff and subsurface runoff (Parchami-Araghi et al. 2013). It determines the distribution of rainfall in karstic surfaces and underground space systems. Rainfall is more likely to enter the underground space through fissures in this area, where surface runoff is difficult to observe (Peng and Wang 2012). However, how does the water infiltration in the near-surface fissures, especially those filled with soils, proceed? It still puzzles us.

Preferential flow is also called non-uniform flow as a common form of soil water movement (Zhang et al. 2019). The pathway distribution characteristics of preferential flow can directly reflect the process of soil water movement. It plays an important role in the water use efficiency of plants and soil water-holding capacity (Sidle et al. 2001; Ma et al. 2017; Hangen et al. 2005). Water in soil usually infiltrates downward with a form of piston flow in the soil matrix (Sukhija et al. 2003), but non-uniform reasons widely distributed in this area, such as animal activities and plant roots in the soil, and also the fissures of soil (Li et al. 2017). The movement of water in soil must be different from that in non-karst areas (Lee et al. 2011). Rock outcrops and soils exhibit mosaic patterns in karst rock desertification areas. There are different hard and soft interfaces between them. Hard interface refers to water repellent rock, and the soft interface refers to permeable soil. Will a new form of soil preferential flow be formed at the rock-soil interface? Solving this problem can further explain why the rock-soil interface in near-surface fissures is one of the ways of water loss in rocky desertification areas.

Therefore, five types of near-surface fissures filled with soils were selected in an area experiencing severe rocky desertification in Guizhou Province, China, to study the

role of the preferential flow at rock–soil interface in the water leaking process in near-surface fissures by using digital image processing technology and the dye tracer method that is most commonly used in preferential flow experiments. This work aims to (i) analyze the pathway distribution characteristics of preferential flow in rock–soil interface, (ii) verify the characteristics of the dyed area ratio of preferential flow in rock-soil interface and (iii) reveal the role of preferential flow in rock–soil interface. The results can further understand the lack of surface runoff and water infiltration of soil in karst rocky desertification areas and discuss the process of the groundwater leakage in this area.

## Materials and methods

### Study site

The study area is located in the town of Qingyan, Huaxi District, Guiyang city, China. Qingyan Town, known as one of the four ancient towns in Guizhou Province, is a typical rocky desertification area in Guiyang. Dr. Marjorie M. Sweeting (1992), an international famous karst geomorphology scientist, had several times come in this area to observe and study karst landform. The town of Qingyan is the central distribution center of the southern suburb, located at 106° 37'- 106°44'E and 26°17'-26°23'N. It is approximately 10 km wide from north to south and 8 km from east to west, with a total area of 92.3 km<sup>2</sup>. The climate of this area belongs to a middle subtropical monsoon humid area. The annual average temperature is 15 °C. The annual average rainfall is approximately 1100 to 1300 mm. The main soil types are calcareous soil on the surface, yellow clay in deeper layer, and paddy soil in the paddy field. These soils are neutral and slightly acidic. The Qingyan River, Yangmei River and Zhaosi River belong to the Pearl River system, which receives an average annual runoff of 613 mm. The Pearl River system has long sources and fine flows and a large fluctuation range of floods and droughts.

### Experimental design

Five types of near-surface fissures were selected to conduct water transport experiments in which no fissures were taken as the control in this area. The near-surface fissures are patches of rock and soil, and the soil at least 1 m away from the rock. The basic information for these near-surface fissures is shown in Table 1. The soil type is calcareous, and the rock type is dolomite. The shape, opening degree and dip angle of the rocks are different at the near-surface fissures. Every plot on an area of 50 cm × 50 cm for each near-surface fissure was selected, and the plant litter and stones on the surface were removed carefully before the test.

**Table 1** Basic information of the selected of near-surface fissures

Numbers	Near-surface fissure types	Opening degree/ degree/cm	Dip angle of rocks/°	Geographic location	/m	Aspect	Vegetations
CK	No fissures	–	–	N26°21'4", E106°40'20"	1069	136°	Corn, Setaria, etc
V	V-type	20	40	N26°21'9", E106°40'18"	1068	100°	Bidens bipinnata, Setaria, etc
W	W-type	38	90	N26°21'8", E106°40'17"	1064	120°	Peach Tree (Height: 153 cm, crown width: 1 m), Bidens bipinnata, Celery, Hispid Arthraxon, etc
WR	-type	40	89	N26°21'8", E106°40'17"	1064	120°	Radish, Ostrich Fern, Rubus parvifolius, Bidens bipinnata, etc
IV	Inclined V-type	53	80	N26°21'9", E106°40'18"	1072	47°	Bidens bipinnata, Chrysanthemum indicum, etc
F	Conduit-type	13	71	N26°21'9", E106°40'17"	1072	123°	Bidens bipinnata, Celtis sinensis, Oxalis, etc

The experiment of soil preferential flow was completed by using Brilliant Blue dye tracer (Flury and Wai. 2003). The dye tracer was Brilliant Blue 85 (Brilliant Blue FCF), and a solution with a concentration of 4 g/L (normal dosage) was prepared as a tracer. Each near-surface fissures type treatment was repeated 3 times. Brilliant Blue FCF with good visibility in the soils is nontoxic and easily adsorbed by soils. It can show the pathway of water movement in near-surface fissures.

## Methods

The test was conducted in July 2020 without a rainfall event. Brilliant blue FCF with a volume of 10 L was sprayed evenly over a 50 cm × 50 cm area at 40 mm/h for each near-surface fissures site. The solution was sprayed manually on the soil surface for approximately 60 min to avoid water accumulation. When the tracer solution had infiltrated (during this period, it was covered with film to reduce the influence of water evaporation and rainfall) after 24 h, the vertical profiles were excavated along the dye boundary at 10 cm intervals (Fig. 1). The excavated depth was limited by the deepest part. The boundary of each profile was determined using a tower ruler. Then, each dyed profile was photographed with a camera (Canon EOS 400 D).

Photograph processing: (i) Cutting the dyed image: The Sect. 10 cm away from both sides of the boundary was removed, taking infiltration depth as the maximum size of the height. (ii) Correcting the dyed image: The parallax problem in the shooting process was corrected, and the image was defined by treating 1 mm × 1 mm as one pixel. (iii) Binary image: The dyed area was colored black, and the

undyed area was colored white through visual inspection methods and the adjustment of the color saturation, color phase, color scale, etc. by using CS5 software. Here, the color difference between the dyed and undyed areas was obvious. The dye-stained area of the images is consistent with the actual. (iv) Statistical image data: Image information statistical analyses were conducted by MATLAB programming, including calculating the black and white dyeing proportion of unit pixel row, drawing the change trend of black and white dyeing proportion with increasing soil depth, and calculating the nonuniformity coefficient, coefficient of variation, and preferential flow parameters.

The dyed area ratio of the profile of preferential flow is widely used to evaluate the degree of preferential flow. The higher the dyeing area ratio is, the more developed the preferential flow (Allaire et al. 2009). This parameter can be calculated by the following formula:

$$D_c = \frac{D}{D + N_D} \quad (1)$$

where  $D_c$  is the ratio of dyed area of a profile;  $D$  is the total dyed area, mm<sup>2</sup>; and  $N_D$  is the undyed area, mm<sup>2</sup>.

The evaluation index of the degree of preferential flow, that is, the variation coefficient of the area ratio or preferential flow (Chen et al. 2015) is used to characterize the relative maturity of preferential flow. It can also directly reflect changes in the dyed area at different depths in the profile. The smaller the evaluation index is, the higher the preferential flow development (Wu et al. 2014; Liang et al. 2017). This parameter can be calculated by the following formula:

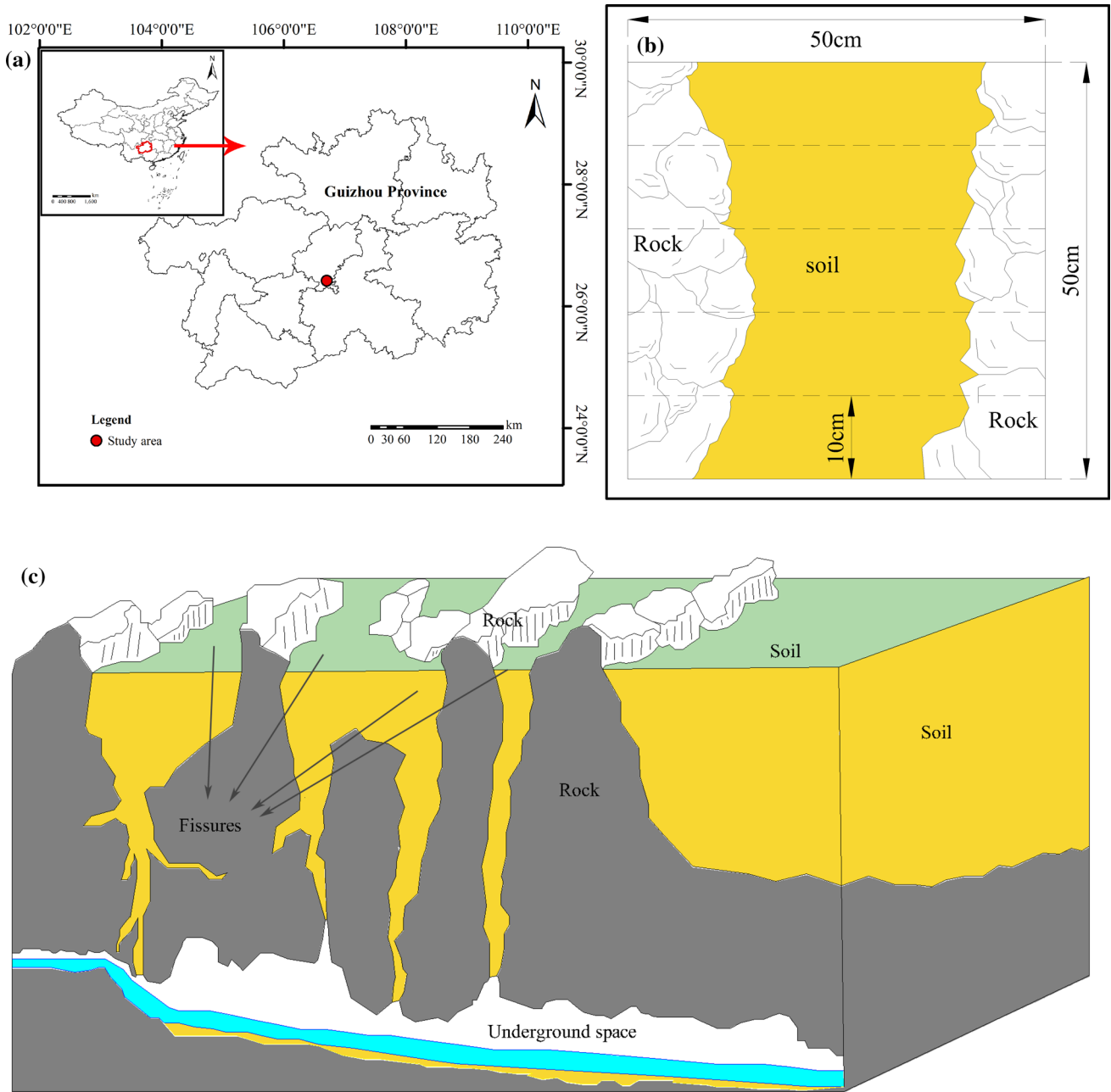


**Fig. 1** Diagrammatic sketch of the dyed profile of near-surface fissures. **a** location of the study site in Guizhou province, China; **b** Rock–soil interface, **c** Different types of near-surface fissures. (CK)

No fissures, (V) V-type fissure, (W) W-type fissure, (WR) W + rocks-type fissure, (IV) inclined V-type fissure, (F) conduit fissure

$$C_v = \frac{S}{\bar{x}} \times 100\% = \frac{\sqrt{\frac{1}{n-1} \sum_{i=1}^n (x_i - \bar{x})^2}}{\frac{1}{n} \sum_{i=1}^n x_i} \times 100\% \quad (2)$$

where  $C_v$  is the variation coefficient, %;  $S$  is the variance in the dyed area ratio;  $\bar{x}$  is the mean value of the dyed area ratio of a profile; and  $x_i$  is the dyed area ratio at the depth of near-surface fissure profile  $i$ .

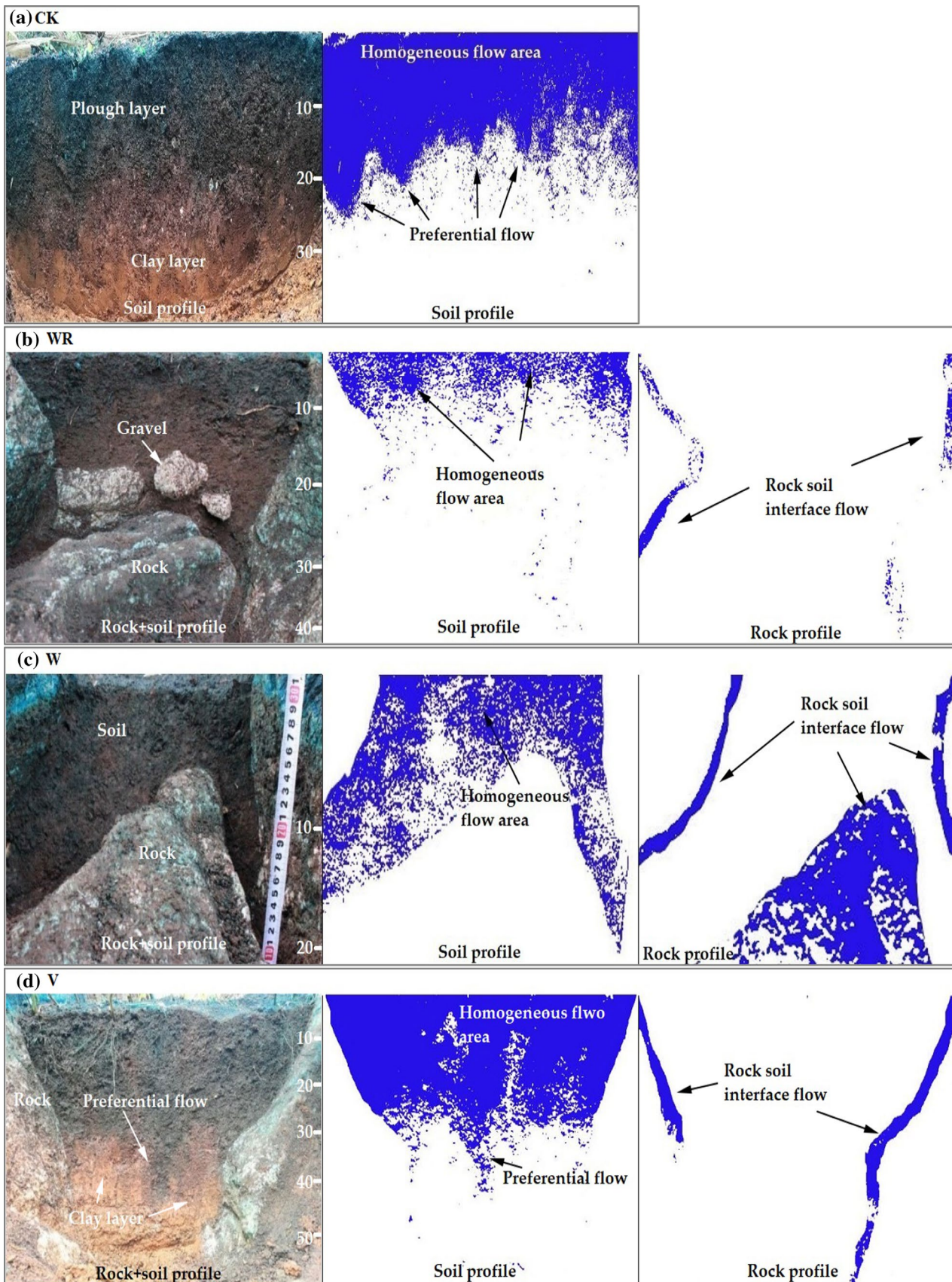


**Fig. 2** Dyed concentration figures of each near-surface fissure in rock + soil, soil and rock profiles. (CK) No fissures, (V) V-type fissure, (W) W-type fissure, (WR) W + rocks-type fissure, (IV) inclined V-type fissure, (F) conduit fissure

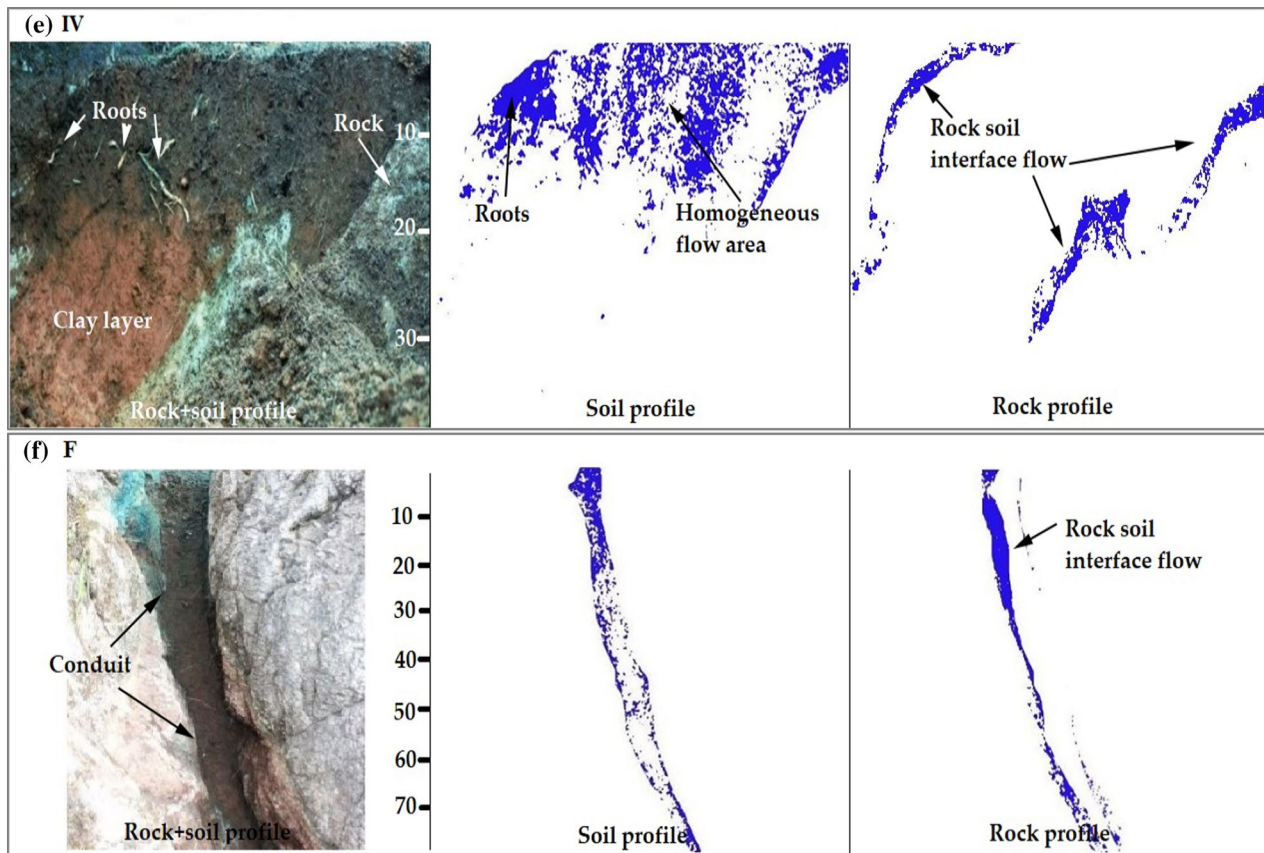


Fig. 2 (continued)

## Results

### Pathway characteristics of preferential flow in rock–soil interface

Figure 2 shows the dyeing characteristics of different near-surface fissure types of rock + soil profile, soil profiles and rock–soil interface. The difference in dyeing concentration of each profile reflects the path of preferential flow or leakage of near-surface fissures. The dyeing of the control (CK) profiles was mainly concentrated in the soil layer 0–30 cm (Fig. 2a). The dyeing shown in the figure is relatively uniform, and the water flow path moves downward in the shape of multiple funnels. Unstained soils are predominantly yellow clay layers with poor permeability, making it difficult for water to pass through. The boundary between the dyed zone and the unstained zone is the junction of the tillage layer and the clay layer. Compared with the control, in the near-surface fissure profile, the dyeing of the preferential flow path is characterized by the path correlation characteristic of the rock–soil interface (Fig. 2b, c, e, f). Among them, the preferential flow dyeing of the V-type near-surface fissure (Fig. 2b) was funnel-shaped, breaking through the yellow

clay layer and reaching a depth of 40 cm. However, the preferential flow path dyeing at the rock–soil interface exceeds 50 cm. Compared with V-type near-surface fissure, the soil–rock interface dyeing of inclined V-type near-surface fissure (Fig. 2e) also breaks through the yellow clay layer. Preferential flow dyeing was also characterized by root-dependent pathways, and dyeing obviously. In contrast, areas with inconspicuous flow dyeing had no or few plant roots. The preferential flow dyeing depth of the conduit-type near-surface fissure profile (Fig. 2f) reaches 70 cm. In the yellow clay layer below 80 cm, it is difficult to observe the dyed part. Unlike other types, the W + rocks-type near-surface fissure contains gravel and is not in contact with the rock–soil interface. The rock–soil interface is dyed but the gravel is not dyed, and the soil interface is also less deeply dyed. This type of near-surface fissure indicates that the preferential flow at the rock–soil interface is faster than that of the soil, allowing water to bypass the soil and preferentially move down through the rock–soil interface path.

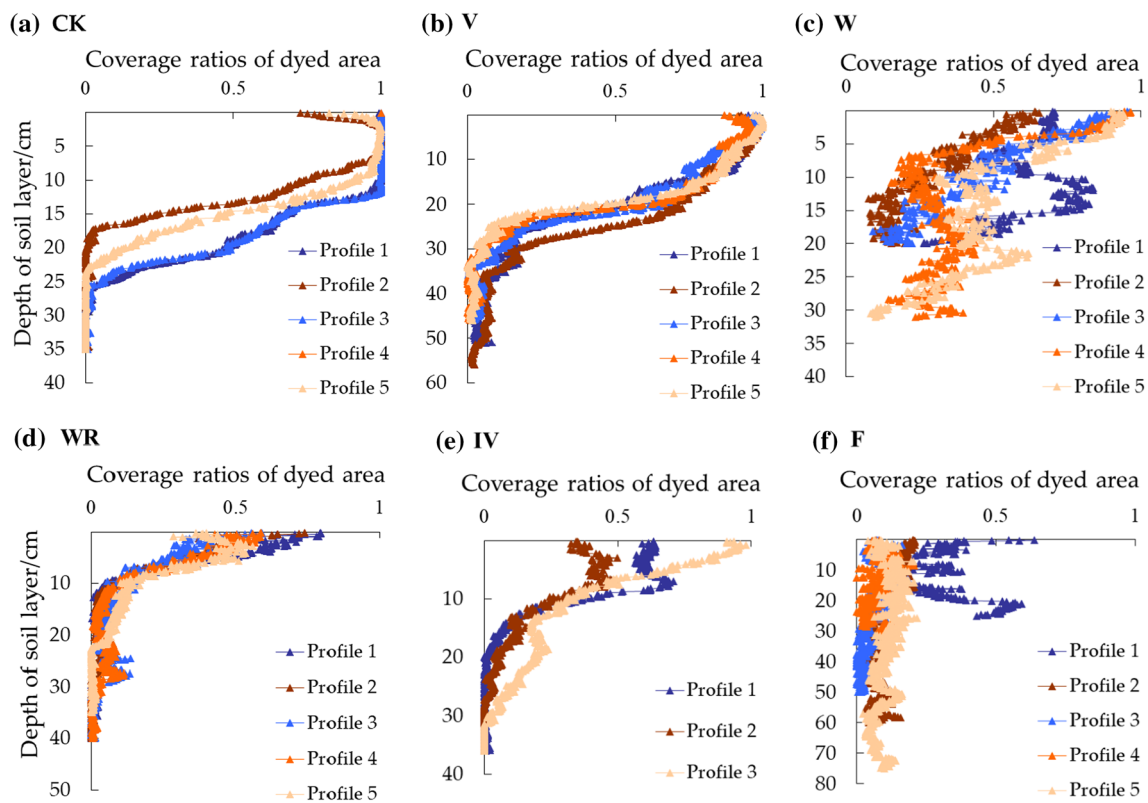


**Fig. 3** Variation in the dyed area ratios of profiles with soil depth for different near-surface fissures. (CK) No fissures, (V) V-type fissure, (W) W-type fissure, (WR) W + rocks-type fissure, (IV) inclined V-type fissure, (F) conduit fissure

**Characteristics of the dyed area ratio of preferential flow in rock-soil interface**

Figure 3 shows the coverage ratios of the dyed area in each profile of the near-surface fissures. With the increase in soil depth, the dyed area ratio of each profile of CK generally increases at first and then decreases (Fig. 3a). The dyed area ratio of each profile is quite different. It decreases sharply at a depth of approximately 7 cm and approaches approximately 0 at 25 cm. There are smaller differences in the dyed area ratio of each profile with the V-type fissure (Fig. 3b). They show a uniform and monotonous sharp decrease in the range of 20–30 cm depth, and then, the dyed area ratio rebounds and tends to zero. The dyed area ratio rebounds at depths of 40–50 cm and subsequently tends to 0 where the rock of rocksoil interface is dyed in this range of soil depths. The changing trend of the dyed area ratio of each profile of W-type near-surface fissure is very different from that of other profiles (Fig. 3c), which related to the distribution of tree roots and gravel in soil (Fig. 2c, there is a peach tree, but the image is not shown due to excavation). Complex soil conditions affect the behavior of water flow, resulting in the complexity of the dyed area ratio of each profile. The dyed area ratio of each profile of W + rock-type near-surface fissure decreases as the soil depth increases (Fig. 3d), but

a double peak rebound appeared in profile 3 at depths of 25 cm and 30 cm. The dyed area ratio of profiles 1 and 2 for the inclined V-type near-surface fissure is obviously different from that of profile 3 within 10 cm in the soil depth, and there is a large difference between each profile (Fig. 3e). The profile 3, which had a downward trend, rebounded at 19 cm and then continued to decline. This is related to the proportion of rock in the profile. In detail, the dyed area of rock is limited to its surface. The three profiles in the image divide the dyed rock area into three parts. In the image field of view, the proportion of rock of profile 1 is the largest, followed by profile 3. In profile 2, because the dyed part of the rock is linear in the profile field of view, the proportion is the smallest. It can be said that the difference of dyed area ratio of each profile is the difference of the dyed area ratio of rock. Differing from the other near-surface fissure conditions, profile 1 of the conduit-type fissure (F) presents a multipeak-valley change obviously within 30 cm in the soil depth (Fig. 3f., The reason for this difference is the same as Fig. 3e). The variation trend of the dyed area ratio for other profiles is gentle in smaller values, which is related to the inclination of the rock and the position of the yellow clay layer (below 70 cm).

The variation characteristics of the average dyed area ratio for each near-surface fissure are presented in Fig. 4.

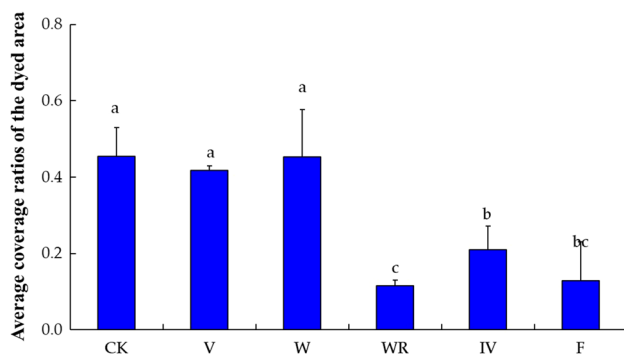


**Fig. 4** Average coverage ratios of the dyed area for different near-surface fissures. (CK) No fissures, (V) V-type fissure, (W) W-type fissure, (WR) W + rocks-type fissure, (IV) inclined V-type fissure, (F) conduit fissure

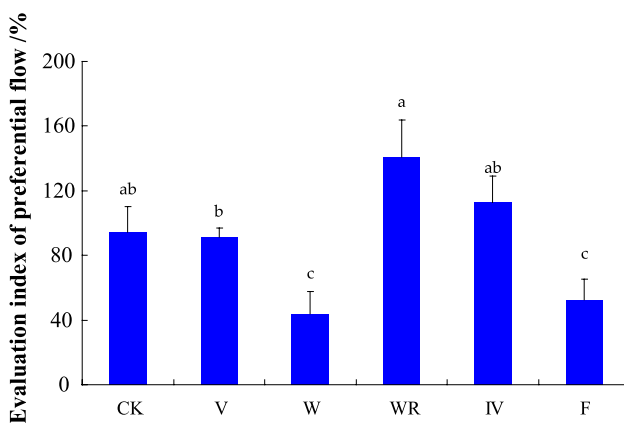


**Fig. 5** Evaluation index of preferential flow for the different near-surface fissures. (CK) no fissures, (V) V-type fissure, (W) W-type fissure, (WR) W + rocks-type fissure, (IV) inclined V-type fissure, (F) conduit fissure

The higher the dye area ratio is, the more developed the preferential flow. The average dyed area ratio of CK is 46%, and the average dyed area ratio of W-type near-surface fissure is 0.45, respectively, which indicates a relatively higher development degree of soil preferential flow. Contrarily, the average dyed area ratios of WR-type, IV-type and conduit (F) fissures are the lowest, indicating a weaker development degree of soil preferential flow. However, that of the preferential flow at the rock–soil interface is well developed (Fig. 2d, e and f).

The variation characteristics of the evaluation index of the degree of preferential flow for each near-surface fissure are shown in Fig. 5. The smaller the evaluation index is, the higher the development of preferential flow. The evaluation index of the degree of preferential flow for each near-surface fissure is in the order of WR (140.63%) > IV

(113.00%) > CK (94.53%) > V (91.44%) > F (52.55%) > W (43.89%). Evidently, the development degree of preferential flow for the conduit (F) and W-type near-surface fissures is the highest.

### The role of preferential flow in the rock–soil interface

The "soil" and "rock" in the near-surface fissures are further distinguished and calculated based on MATLAB program. The dyed area ratio of the rock + soil profile, only the soil profile and only the rock profile is shown in Fig. 6. The variation trends of the rock + soil profile and soil profile of the W-type near-surface fissure are quite different, while the other types have little difference. The variation trend of the dyeing area ratio of the rock–soil interface of various types of near-surface fissures is very different from that of the rock + soil profile and the soil profile. With the increase in soil depth, the variation range of the dyed area ratio of the rock–soil interface is smaller (dyed area ratio < 0.2, except for W type), while the variation range of rock + soil profile and soil profile is larger (except for F type, dyed area ratios are between 0 and 1). The variation trend of rock + soil profile, soil profile and rock–soil interface dyeing area ratio of conduit type (F) surface fissure is small, indicating that the preferential flow of rock–soil interface plays an important role in this type. Combined with the characteristics of the actual excavation profile (Fig. 2), the difference in the staining area ratio between the soil profile and the rock–soil interface shows that the main migration mode of preferential flow at the rock–soil interface is vertical infiltration. As soil depth increases, preferential flow at the rock–soil interface dominates water movement in near-surface fissures.

Table 2 shows the statistical characteristics of the dyed area ratio of the rock + soil, soil profiles and rock–soil interface. The dyed area ratio of preferred flow for each rock + soil profile varies from 0.12 to 0.48, that of the soil profile varies from 0.06 to 0.37, and that of the rock–soil interface varies from 0.02 to 0.16. The rock–soil interface consistently presents the smallest values in the dyed area ratio and lowest variation range for preferential flow. The evaluation indexes of the degree of preferential flow in the rock + soil profile, the soil profile and the rock–soil interface change in the ranges of 43.9%–113%, 74.1%–144.4% and 49.3%–105.7%, respectively. Obviously, the rock + soil profile ranks highest in the variation of evaluation index, followed by the soil profile; the rock–soil interface is still the smallest. Although the proportion of rock–soil interface in the dyed area of the profile is very small, the preferential flow of rock–soil interface is still the main form of preferential flow in the near-surface fissures.



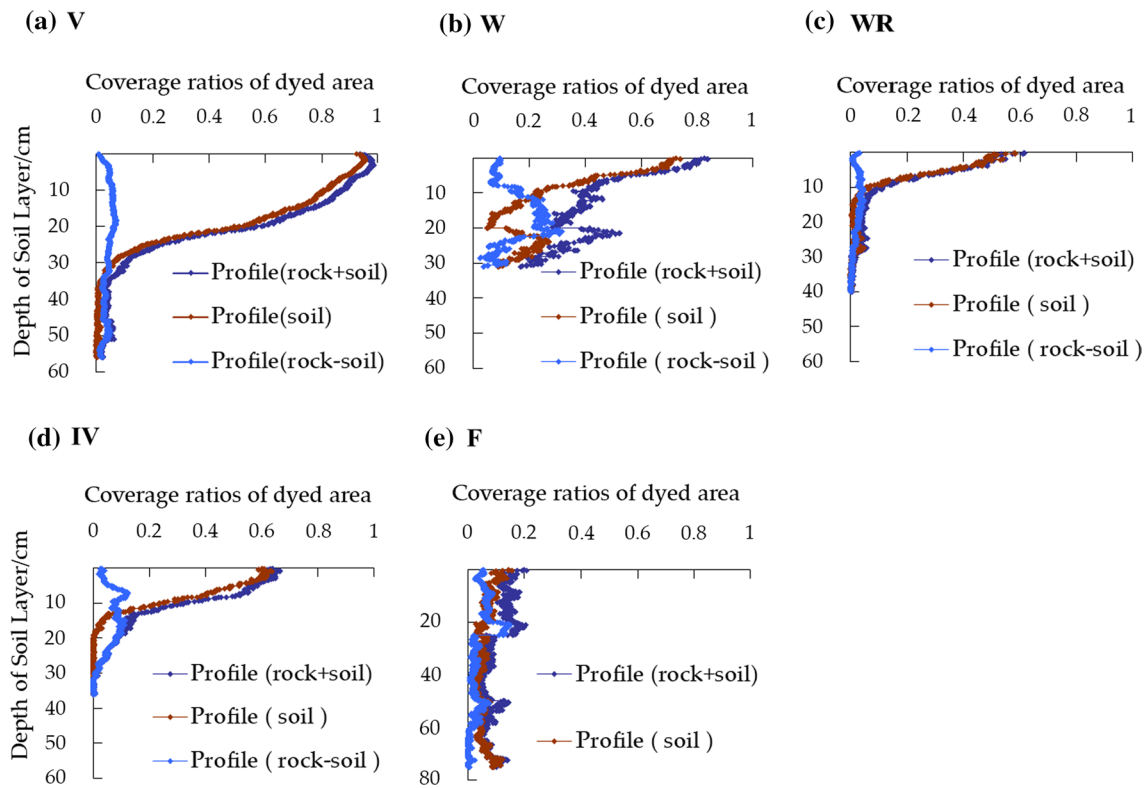


**Fig. 6** Coverage ratios of dyed area in rock + soil, soil and rock–soil profiles. (V) V-type fissure, (W) W-type fissure, (WR) W + rocks-type fissure, (IV) inclined V-type fissure, (F) conduit fissure

**Table 2** Statistical characteristics of the dyed area ratio of profiles of different near-surface fissures

Near-surface fissure numbers	Rock + soil profile		Soil profile		Rock–soil profile	
	The dyed area ratio of preferential flow	Evaluation index of the degree of preferential flow (%)	The dyed area ratio of preferential flow	Evaluation index of the degree of preferential flow (%)	The dyed area ratio of preferential flow	Evaluation index of the degree of preferential flow (%)
V	0.42 a	94.5 b	0.37 a	100.0 b	0.04 bc	49.3 c
W	0.45 a	91.4 b	0.29 a	83.9 c	0.16 a	59.4 bc
WR	0.12 b	43.9 c	0.09 c	169.3 a	0.02 c	80.8 ab
IV	0.48 a	112.0 a	0.15 b	144.4 a	0.06 b	105.7 a
F	0.13 b	113.0 a	0.06 c	74.1 c	0.07 b	78.0 b

LSD (Least Significant Different) method was used for multiple comparisons. Different lowercase letters in the same column showed significant difference ( $P < 0.05$ ), while the same letters showed no significant difference ( $P > 0.05$ )

## Discussion

### Pathway analysis of preferential flow in rock–soil interface

Water in soil usually infiltrates downward with a form of piston flow in the soil matrix (Sukhija et al. 2003). Therefore, the depth of soil water infiltration mainly depends on rainfall and soil bottom conditions in control (CK). The clay layer at

the bottom of the soil hindered the movement downward of water, and the dyed area decreased sharply at the junction of the clay layer and the tillage layer, approaching 0. However, the mosaic distribution of rocks and soils is the largest feature on the surface in rocky desertification areas. This results in the formation of hard and soft interfaces between rock and soil (Ackermann et al. 2013). These interfaces provide a preferential channel for water movement by connecting the tillage layer with good permeability and the clay layer

with poor permeability (Zhao et al. 2020). As this study shows, water flows preferentially at the rock–soil interface, which dominates the water movement in near-surface fissures (Sohrt et al. 2014). The depth of water infiltration at rock–soil interface is more than that in the soil interface. Caves of animals in soil and holes of plant roots are also the reasons for preferential flow of water in soil (Li et al. 2017; Zhang et al. 2016). In this study, the soil at the plant roots showed root-related dyed characteristics (Fig. 2e), but the traces of caves were not obvious. Roots provide preferential access and promote water infiltration (Helliwell et al. 2017). Studies have shown that the content of organic carbon at the rock–soil interface is higher, while the content of clay is far lower than that of the soil far away from the rock–soil interface (Sohrt et al. 2014). This is one of the reasons for the deep infiltration of water at the rock–soil interface. But this is the contribution to the water leakage only at the rock–soil interface. In contrast, plant roots act on soil near-surface fissures. The effect of root system on preferential flow was limited to a part (Fig. 2e) when the range of root system is small. Peach is one of the plant types in W-type near-surface fissure. The root system of peach changed the physical properties of soil (e.g., increasing soil aggregates and organic carbon) (Cerdà. 1998; Hartemink et al. 2006). It can increase the soil porosity (Benegas et al. 2014) and increase soil permeability. Combined with the preferential flow pathway of rock–soil interface, the water movement of this type (W) fissure is very different from other types. The variation of dyed area ratio is very irregular for each profile of W-type near-surface fissure (Fig. 3c). The dyed area ratio is the largest, and the evaluation index of preferential flow is the smallest (Figs. 4 and 5). Preferential flow of this type of near-surface fissure is well developed. However, the dyed characteristics of water infiltration are discontinuous in conduit fissure (F). On the one hand, it may be related to the narrow area, thin soil cover and deeper clay layer (Zhao et al. 2018), on the other hand, it may be related to the almost vertical dip angle of rock (Fleury et al. 2007; Zhang et al. 2011a, b), which increases the role of water flow in the vertical direction. These reasons lead to the underground infiltration speedy of preferential flow in this type of near-surface fissure, which greatly shortens the time of water infiltration (Romanov et al. 2011). Although the dyed area ratio of preferential flow is the smallest in this type, the depth of dyed characteristics (up to 70 cm deep) indicates that the preferential flow at the rock–soil interface is very developed.

### Influencing factors of the formation of rock–soil interface flow

Previous studies (Nobles et al. 2010; Zhao et al. 2020; Guo et al. 2019; Fu et al. 2015) have studied the water flow behavior of karst slopes by simulating rainfall, dye tracing,

and ground-penetrating radar. The results show that water flow behavior mainly occurs at the rock–soil interface in the form of preferential flow, which is mainly affected by the fluctuation of underlying bedrock, structure of soil and rock, etc. Previous studies have shown that if the rainfall is large and the runoff is fully accumulated, and the infiltration rate is lower than the production rate, surface runoff and soil flow will occur at the same time (Zhang et al. 2011a, b). In this study, the rock–soil interface changed the continuity of the yellow clay layer, the soil preferential flow infiltrated along the channel of the rock–soil interface, and the preferential flow of the rock–soil interface dominated the water transport form of near-surface fissures, which also proved this conclusion. The continuity of soil matrix was changed. Because of the agglomerative nature of the soil, it is easy to dry and shrink to form fissures (Haria et al. 1994). The rock–soil interface becomes a preferential channel for water transport in near-surface fissures. The fissure changes the generation mechanism of flow and pathway characteristics of near-surface fissures and provides an opportunity for water leakage to the bottom of soil. Researchers found that plant roots and caves are involved in the process of preferential flow at the rock–soil interface (Zhao et al. 2018), which has a significant contribution to the development of preferential flow. The fissures of rock–soil interface and the process of water leakage to the bottom of soil and provide the conditions for plant roots and other living beings to expand to the bottom of soil, such as air and water (Ackermann et al. 2013). Biological activities increase the porosity of the soil in near-surface fissures, thus increasing the permeability of soil (Beven and Germann 2013). This is a process of positive correlation. In this study, it is found that the continuity and leakage direction of flow of rock–soil interface affected by the size and direction of rock. There are few related studies. In fact (Fig. 2e and f., Fig. 3e and f., described in the text above), the rock is confined to its surface because of water repellency, and the dyed area is divided into three parts by each profile be excavated. In the image field of view, the rock dyed area ratio determined the dyed area ratio in each profile. Therefore, we consider rock shape, inclination, and size as influencing factors of the formation of rock–soil interface flow. There are gravel, longitudinal and transverse large-scale rocks distributed in the near-surface fissure of WR type. These factors have different meanings to the rock–soil interface flow. The role of gravel should be characterized by local water infiltration, and the larger longitudinal rock at the bottom will transfer water to the bottom of soil. The dyeing characteristics of transverse rocks indicate that the transverse flow occurs at the rock–soil interface (Li et al. 2017; Zhao et al. 2020; Cerdà 2010; Abrahams and Parsons 1991). This is related to the hydrophobic effect of the rock, where the water is blocked, flows along the rock until it meets the leakage pathway, and then leaks to the bottom of the soil. The

dyed characteristics of pipe fissure F (up to 70 cm depth, the deepest one in all near-surface fissures) (Fig. 2f) showed that the development of rock–soil interface flow is related to the distribution of clay layer below the depth of 70 cm and the area ratio of rock and water redistribution (Dai et al. 2017). Due to less soil and high permeability, large rock and dip angle, etc., the water quickly infiltrates into the underground space. The retention time of water in soil and rock vertically distributed in the profile of 30 cm–70 cm is too short, or it directly bypasses the pathway. As a result, the dyeing of rock and soil in 30 cm–70 cm is not obvious, while that in 0–30 cm and 70 cm depth is obvious. Therefore, under certain rainfall conditions, the development degree of preferential flow at rock–soil interface depends on the bottom conditions of soil of the near-surface fissures (rock, plant roots, etc.).

### **Influence of preferential flow at the rock–soil interface on underground leakage of water**

There is a special dual surface and underground structure in the karst rocky desertification area. The special rock–soil interface makes the surface and underground hydrological processes more complex and unique in karst areas (Li et al. 2016). Compared with CK, the preferential flow of soil in near-surface fissures has the advantage of downward leakage, when rainfall water infiltrates past the rock–soil interface, it produces lateral preferential flow along the interface. The interaction of the preferential flow in the horizontal and vertical directions causes rapid water infiltration through the cracks at the rock–soil interface (Germann and Zimmermann 2005). The depth of water movement is much deeper than CK. This indicates that the rock–soil interface provides a fast channel for surface water to move into the underground space system, and the water enters the underground space along the rock–soil interface (Cao et al. 2007). Therefore, preferential flow at rock–soil interface is considered to be the dominant type of water movement in hillslope (Jaromir and Tomas 2018). Essentially, the reason for the preferential leakage of water at the rock–soil interface is that the carbonate rocks are easily dissolved and have significant differential dissolution (Herman et al. 2012). In addition, the boundary of the rock–soil interface is clear and abrupt (Zhang et al. 2011a, b; Walter et al. 1995), forming a rapid channel for water migration. Moreover, rock is impermeable, and the water flows along preferential channels, forming the preferential flow and rapidly leaking into the underground space. Compared with CK, preferential flow infiltrates rapidly at the rock–soil interface with fewer paths and even contributes to a higher water leakage (Sohrt et al. 2014). In other words, there is an evident difference in the water infiltration rate between the rock-soil interface in near-surface fissures and the soil in CK. The characteristics of preferential infiltration of the rock-soil interface of WR-type near-surface fissure indicate

that the infiltration characteristics of the rock-soil interface in near-surface fissures are different from that of the surrounding soil (Zhao et al. 2018). As a result, the infiltration rate of rock-soil interface is higher than that of surrounding soil and CK, preferential flow at the rock–soil interface penetrates faster and deeper, which raises the water leakage rate from the karst area. In this study, a sudden decrease in dyed area appears in the fissure F. It is certain that the infiltration speed of this type of rock-soil interface flow is faster and the infiltration depth is deeper than other types of near-surface fissures. The water movement directly bypasses the soil near the surface fissure and is guided to the 70 cm position where the yellow clay layer is located. The preferential flow of ultrafast infiltration reduces soil water storage (Wang et al. 2014). Rainfall is introduced into the ground in the form of preferential flow, so the surface runoff is rarely observed in karst areas. Rock–soil interface is widely distributed in karst rocky desertification area, and soil distribution is fractured. Preferred flow at rock-soil interface is also widely distributed, and migration capacity of preferential flow is stronger than that of matrix flow (Kan et al. 2019). However, whether preferential flow at the rock-soil interface drives soil downward leakage remains to be studied. As a result, on one hand, water leakage rapidly in karst rocky desertification area significantly reduces soil water-holding capability in this area, where the rapid loss of water causes special rocky desertification drought in this area, which makes it difficult for plants to use water (Li et al. 2016; Kan et al. 2019). On the other hand, preferential flow at the rock–soil interface increases the water supply at the bottom of soil in near-surface fissures, which is good for the growth of plant at the bottom of soil (Lesschen et al. 2008; Danin 1999; Zhao et al. 2020). Plant roots increase soil pores, form a new pathway of preferential flow, and cause rapid infiltration of rainwater (Valverde et al. 2015; Kai et al. 2012). Rock–soil interface has advantages in guiding preferential flow and replenishing groundwater. In the karst rocky desertification area, the soil exhibits a strong infiltration capacity, and the rock surface can rapidly produce runoff (Li et al. 2011). Both of these conditions enhance rapid infiltration into the underground space at the rock–soil interface. This unique preferential flow is much faster than traditional macropore preferential flow in soil (Sidle et al. 2001). Therefore, the preferential flow at the rock-soil interface may be one of the reasons for driving the surface erosion and soil leakage in the near-surface fissures and further aggravate the process of rocky desertification in karst areas (Yang et al. 2011; Chen et al. 2012; Peng et al. 2016).

### **Conclusions**

In the present study, we have shown that the water flow at the rock-soil interface is the main preferential flow type in the near-surface fissures. The variation range of the staining area

ratio of the rock + soil profile was 0.12~0.48, the soil profile was 0.06~0.37, and the rock–soil interface was 0.02~0.16. The dyed area ratio and variation range of the rock–soil interface are the smallest. However, the rock–soil interface provides a transport pathway for the development of preferential flows in the region. Soil preferential flow can pass through poorly permeable clay layers along the rock–soil interface. In this study, the W-type near-surface fissure had the most developed soil preferential flow, with a staining area ratio of 0.45, and the soil preferential flow evaluation index was 43.9%. The dyeing area ratio of other types of near-surface fissures is between 0.04 and 0.07, and the evaluation index of preferential flow degree is between 49 and 106%. These types of preferential flows are underdeveloped in soil, but very well developed at the rock–soil interface. The soil preferential flow flows to the deeper soil layer through the preferential channel of the rock–soil interface in the form of rock–soil interface flow. This is one of the important factors of water leakage in this area.

**Funding** This work was supported by the Science and Technology Plan Project of Guizhou Province (Qian Ke He Ji Chu [2020]1Y176), the National Natural Science Foundation of China (NO. 42007067), the First Class Discipline Construction Projects of Guizhou Province (GNYL[2017]007), the Young Scientific and Technological Talents Growth Project in Colleges and University of Guizhou Province (Qian Ke Jiao KY Zi [2021]082), and the National Natural Science Foundation Training Program for Young Teachers at Guizhou University (Gui Da Pei Yu [2019]36).

## Declarations

**Conflict interest** This work does not have any conflict of interest.

**Open Access** This article is licensed under a Creative Commons Attribution 4.0 International License, which permits use, sharing, adaptation, distribution and reproduction in any medium or format, as long as you give appropriate credit to the original author(s) and the source, provide a link to the Creative Commons licence, and indicate if changes were made. The images or other third party material in this article are included in the article's Creative Commons licence, unless indicated otherwise in a credit line to the material. If material is not included in the article's Creative Commons licence and your intended use is not permitted by statutory regulation or exceeds the permitted use, you will need to obtain permission directly from the copyright holder. To view a copy of this licence, visit <http://creativecommons.org/licenses/by/4.0/>.

## References

- Abrahams AD, Parsons AJ (1991) Relation between infiltration and stone cover on a semiarid hillslope, southern Arizona. *J Hydrol* 122:49–59. [https://doi.org/10.1016/0022-1694\(91\)90171-D](https://doi.org/10.1016/0022-1694(91)90171-D)
- Ackermann O, Zhevelev HM, Svoray T (2013) *Sarcopoterium spinosum* from mosaic structure to matrix structure: Impact of calcrete (Nari) on vegetation in a Mediterranean semi-arid landscape. *CATENA* 101:79–91. <https://doi.org/10.1016/j.catena.2012.10.001>
- Allaire SE, Roulier S, Cessna AJ (2009) Quantifying preferential flow in soils: a review of different techniques. *J Hydrol* 378(1–2):179–204. <https://doi.org/10.1016/j.jhydrol.2009.08.013>
- Benegas L, Ilstedt U, Roupsard O, Jones J, Malmer A (2014) Effects of trees on infiltrability and preferential flow in two contrasting agroecosystems in central America. *Agric Ecosyst Environ* 183:185–196. <https://doi.org/10.1016/j.agee.2013.10.027>
- Beven K, Germann P (2013) Macropores and water flow in soils. *Water Resour Res* 18(5):1311–1325. <https://doi.org/10.1002/wrcr.20156>
- Cao JS, Zhang WJ, Liu CM, Yang YH (2007) Unsaturated seepage characteristics in the slope characterized by a weathered rock–soil dual entity. *Trans Chin Soc Agric Eng* 23(8):9–15. [https://doi.org/10.1016/S1872-5813\(08\)60001-8](https://doi.org/10.1016/S1872-5813(08)60001-8)
- Cerdà A (1998) The influence of geomorphological position and vegetation cover on the erosional and hydrological processes on a Mediterranean hillslope. *Hydrol Processes* 12:661–667. [https://doi.org/10.1002/\(SICI\)1099-1085\(19980330\)12:4%3c661::AID-HYP607%3e3.0](https://doi.org/10.1002/(SICI)1099-1085(19980330)12:4%3c661::AID-HYP607%3e3.0)
- Cerdà A (2010) Effects of rock fragment cover on soil infiltration, interrill runoff and erosion. *Eur J Soil Sci* 52(1):59–68. <https://doi.org/10.1046/j.1365-2389.2001.00354.x>
- Chen H, Yang J, Fu W, He F, Wang K (2012) Characteristics of slope runoff and sediment yield on karst hill-slope with different land-use types in northwest Guangxi. *Trans Chin Soc Agric Eng* 28(16):121–126. <https://doi.org/10.3969/j.issn.1002-6819.2012.16.019> ((in Chinese))
- Chen HS, Nie YP, Wang KL (2013) Spatio-temporal heterogeneity of water and plant adaptation mechanisms in karst regions: a review. *Acta Ecol Sin* 33(2):317–326. <https://doi.org/10.5846/stxb201112011836> ((in Chinese))
- Chen X, Zhang H, Cheng J, Zhang F, Ruan X (2015) Quantitative evaluation of preferential flow development degree based on dyed image variability analysis. *Trans Chin Soc Agric Eng* 46(5):93–100. <https://doi.org/10.6041/j.issn.1000-1298.2015.05.014>
- Dai QH, Peng XD, Yang Z, Zhao LS (2017) Runoff and erosion processes on bare slopes in the Karst Rocky Desertification Area. *CATENA* 152:218–226. <https://doi.org/10.1016/j.catena.2017.01.013>
- Danin A (1999) Sandstone outcrops—a major refugium of Mediterranean flora in the xeric part of Jordan. *Isr J Plant Sci* 47:179–187. <https://doi.org/10.1080/07929978.1999.10676771>
- Fleury P, Plagnes V, Bakalowicz M (2007) Modelling of the functioning of karst aquifers with a reservoir model: Application to Fontaine de Vaucluse (South of France). *J Hydrol* 345(1–2):38–49. <https://doi.org/10.1016/j.jhydrol.2007.07.014>
- Flury M, Wai NN (2003) Dyes as tracers for vadose zone hydrology. *Rev Geophys* 41(1):1002. <https://doi.org/10.1029/2001RG000109>
- Fu ZY, Chen HS, Zhang W, Xu QX, Wang S, Wang KL (2015) Subsurface flow in a soil-mantled subtropical dolomite karst slope: a field rainfall simulation study. *Geomorphol* 250:1–14. <https://doi.org/10.1016/j.geomorph.2015.08.012>
- Germann PF, Zimmermann M (2005) Directions of preferential flow in a hillslope soil, 1 quasi-steady flow. *Hydrol Process* 19:887–899. <https://doi.org/10.1002/hyp.1506>
- Guo L, Lin H, Fan B, Nyquist J, Toran L, Mount G (2019) Preferential flow through shallow fractured bedrock and a 3D fill-and-spill model of hillslope subsurface hydrology. *J Hydrol* 576:430–442. <https://doi.org/10.1016/j.jhydrol.2019.06.070>
- Hangen E, Gerke HH, Schaaf W, Hüttl RF (2005) Assessment of preferential flow processes in a forest-reclaimed lignitic mine soil by multicell sampling of drainage water and three tracers. *J Hydrol* 303(1):16–37. <https://doi.org/10.1016/j.jhydrol.2004.07.009>

- Haria AH, Johnson AC, Bell JP, Batchelor CH (1994) Water movement and isotoproturon behaviour in a drained heavy clay soil: 1 preferential flow processes. *J Hydrol* 163(3–4):203–216. [https://doi.org/10.1016/0022-1694\(94\)90140-6](https://doi.org/10.1016/0022-1694(94)90140-6)
- Hartemink AE, Veldkamp T, Bai Z (2006) Land cover change and soil fertility decline in tropical regions. *Turk J Agric* for 32:195–213. <https://doi.org/10.1590/S0103-90162008000600016>
- Helliwell JR, Sturrock CJ, Mairhofer S, Craigon J, Ashton RW, Miller AJ, Whalley WR, Mooney SJ (2017) The emergent rhizosphere: imaging the development of the porous architecture at the root-soil interface. *Sci Rep* 7(1):14875. <https://doi.org/10.1038/s41598-017-14904-w>
- Herman EK, Toran L, White WB (2012) Clastic sediment transport and storage in fluvio-karst aquifers: an essential component of karst Hydrogeology. *Carbonates Evaporites* 27(3–4):211–241. <https://doi.org/10.1007/s13146-012-0112-7>
- Jaromir D, Tomas V (2018) Hillslope hydrograph separation: the effects of variable isotopic signatures and hydrodynamic mixing in macroporous soil. *J Hydrol* 563:446–459. <https://doi.org/10.1016/j.jhydrol.2018.05.054>
- Kai S, Ebermann S, Schalling N (2012) Evidence of double-funneling effect of beech trees by visualization of flow pathways using dye tracer. *J Hydrol* 470–471:184–192. <https://doi.org/10.1016/j.jhydrol.2012.08.048>
- Kan X, Cheng J, Hu X, Zhu F, Li M (2019) Effects of grass and forests and the infiltration amount on preferential flow in Karst Regions of China. *Water* 11(8):1634. <https://doi.org/10.3390/w11081634>
- Lee ML, Kassim A, Gofar N (2011) Performances of two instrumented laboratory models for the study of rainfall infiltration into unsaturated soils. *Eng Geol* 117(1–2):78–89. <https://doi.org/10.1016/j.enggeo.2010.10.007>
- Lesschen JP, Cammeraat LH, Kooijman AM, Wesemael BV (2008) Development of spatial heterogeneity in vegetation and soil properties after land abandonment in a semi-arid ecosystem. *J Arid Environ* 72:2082–2092. <https://doi.org/10.1016/j.jaridenv.2008.06.006>
- Li XY, Contreras S, Solé-Benet A, Cantón Y, Domingo F, Lázaro R, Lin H, Wesemael BV, Puigdefàbregas J (2011) Controls of infiltration-runoff processes in Mediterranean karst rangelands in SE Spain. *CATENA* 86(2):98–109. <https://doi.org/10.1016/j.catena.2011.03.003>
- Li S, Birk S, Xue L, Ren HD, Chang J, Yao XH (2016) Seasonal changes in the soil moisture distribution around bare rock outcrops within a karst rocky desertification area (Fuyuan County, Yunnan Province). *China Environ Earth Sci* 75(23):1482. <https://doi.org/10.1007/s12665-016-6290-1>
- Li B, Pales AR, Clifford HM, Kupis S, Hennessy S, Liang W, Moysey S, Powell B, Finneran KT, Darnault CJG (2017) Preferential flow in the vadose zone and interface dynamics: impact of microbial exudates. *J Hydrol* 558:72–89. <https://doi.org/10.1016/j.jhydrol.2017.12.065>
- Liang J, Wu Y, Zhou J, Wang J, Li R (2017) Quantitative evaluation of effect of soil types on preferential flow pathways and soil phosphorus forms. *Trans Chin Soc Agric Mach* 48(1):220–227. <https://doi.org/10.6041/j.issn.1000-1298.2017.01.029>
- Liu Y, Liu C, Rubinato M, Guo K, Cui M (2020) An assessment of soil's nutrient deficiencies and their influence on the restoration of degraded karst vegetation in Southwest China. *Forests* 11(8):797. <https://doi.org/10.3390/f11080797>
- Ma B, Liang X, Liu S, Jin M, Nimmo JR, Li J (2017) Evaluation of diffuse and preferential flow pathways of infiltrated precipitation and irrigation using oxygen and hydrogen isotopes. *Hydrogeol J* 25(3):675–688. <https://doi.org/10.1007/s10040-016-1525-5>
- Nobles MM, Wilding LP, Lin HS (2010) Flow pathways of bromide and brilliant blue FCF tracers in caliche soils. *J Hydrol* 393:114–122. <https://doi.org/10.1016/j.jhydrol.2010.03.014>
- Oberle P, Ikhwan M, Stoffel D, Nestmann F (2016) Adapted hydro-power-driven water supply system: assessment of an underground application in an Indonesian karst area. *Appl Water Sci* 6:259–278. <https://doi.org/10.1007/s13201-016-0425-0>
- Parchami-Araghi F, Mirlatifi SM, Ghorbani Dashtaki S, Mahdian MH (2013) Point estimation of soil water infiltration process using artificial neural networks for some calcareous soils. *J Hydrol* 481:35–47. <https://doi.org/10.1016/j.jhydrol.2012.12.007>
- Peng T, Wang SJ (2012) Effects of land use, land cover and rainfall regimes on the surface runoff and soil loss on karst slopes in southwest China. *CATENA* 90(1):53–62. <https://doi.org/10.1016/j.catena.2011.11.001>
- Peng XD, Dai QH, Yang Z, Zhao LS (2016) Sediment yield of surface and underground erosion in the process of Rocky Desertification of Karst Area. *Acta Pedol Sin* 53(5):1237–1248. <https://doi.org/10.11766/trxb201601110565> ((in Chinese))
- Romanov D, Kaufmann G, Hiller T (2011) Karstification of aquifers interspersed with non-soluble rocks: from basic principles towards case studies. *Eng Geol* 116(3–4):261–273. <https://doi.org/10.1016/j.enggeo.2010.09.008>
- Sidle RC, Shoji N, Yoshio T, Karin L (2001) A conceptual model of preferential flow systems in forested hillslopes: evidence of self-organization. *Hydrol Process* 15(10):1–18. <https://doi.org/10.1002/hyp.233>
- Sohrt J, Ries F, Sauter M, Lange J (2014) Significance of preferential flow at the rock soil interface in a semi-arid karst environment. *CATENA* 123:1–10. <https://doi.org/10.1016/j.catena.2014.07.003>
- Song XW, Gao Y, Green SM, Dungait JAJ, Peng T, Quine TA, Xiong BL, Wen XF, He NP (2017) Nitrogen loss from karst area in China in recent 50 years: an in-situ simulated rainfall experiment's assessment. *Ecol Evol* 7(23):10131–10142. <https://doi.org/10.1002/ece3.3502>
- Sukhija BS, Reddy DV, Nagabhushanam P, Hussain S (2003) Recharge processes: piston flow vs preferential flow in semi-arid aquifers of India. *Hydrogeol J* 11(3):387–395. <https://doi.org/10.1007/s10040-002-0243-3>
- Sweeting M (1992) Tectonics and fluvial denudation in the formation of cone karst, with particular reference to South China. *Tübinger Geogr Stud* 109:45–56
- Valverde A, Makhallanyane TP, Seely M, Cowan DA (2015) Cyanobacteria drive community composition and functionality in rock-soil interface communities. *Mol Ecol* 24(4):812–821. <https://doi.org/10.1111/mec.13068>
- Walter AV, Nahon D, Flicoteaux R, Girard JR, Melfi A (1995) Behaviour of major and trace elements and fractionation of REE under tropical weathering of a typical apatite-rich carbonatite from Brazil. *Earth Planet Sci Lett* 136(3–4):591–602. [https://doi.org/10.1016/0012-821X\(95\)00195-1](https://doi.org/10.1016/0012-821X(95)00195-1)
- Wang J, Zou B, Liu Y, Tang Y, Zhang X, Yang P (2014) Erosion-creep-collapse mechanism of underground soil loss for the karst rocky desertification in Chenqi village, Puding county, Guizhou China. *Environ Earth Sci* 72(8):2751–2764. <https://doi.org/10.1007/s12665-014-3182-0>
- White WB (2002) Karst hydrology: recent developments and open questions. *Eng Geol* 65(2):85–105. [https://doi.org/10.1016/S0013-7952\(01\)00116-8](https://doi.org/10.1016/S0013-7952(01)00116-8)
- White WB, Culver DC, Herman JS (1995) Karst Lands: the dissolution of carbonate rock produces unique landscapes and poses significant Hydrological and environmental concerns. *Am Sci* 7(5):362–362
- Wu Q, Zhang J, Lin W, Wang G (2014) Applying dyeing tracer to investigate patterns of soil water flow and quantify preferential flow in soil Columns. *Trans Chin Soc Agric Eng* 30(07):82–90 ((in Chinese))
- Yang P, Tang YQ, Zhou NQ, Wang JX, She TY, Zhang XH (2011) Characteristics of red clay creep in karst caves and loss leakage of soil in the karst rocky desertification area of Puding County, Guizhou China. *Environ Earth Sci* 63(3):543–549. <https://doi.org/10.1007/s12665-010-0721-1>

- Zhang DF, Wang SJ, Zhou DQ, Li RL (2001) Intrinsic driving mechanism of land rocky desertification in karst regions of guizhou province. *Bull Soil Water Conserv* 21(4):1–5. <https://doi.org/10.13961/j.cnki.stbctb.2001.04.001> (in Chinese)
- Zhang X, Bai X, He X (2011a) Soil creeping in the weathering crust of carbonate rocks and underground soil losses in the karst mountain areas of Southwest China. *Carbonates Evaporites* 26(2):149–153. <https://doi.org/10.1007/s13146-011-0043-8>
- Zhang Z, Xi C, Ghadouani A, Peng S (2011b) Modelling hydrological processes influenced by soil, rock and vegetation in a small karst basin of southwest China. *Hydrol Process* 25(15):2456–2470. <https://doi.org/10.1002/hyp.8022>
- Zhang Y, Zhang M, Niu J, Zheng H (2016) The preferential flow of soil: a widespread phenomenon in pedological perspectives. *Eurasian Soil Sci* 49:661–672. <https://doi.org/10.1134/S1064229316060120>
- Zhang J, Lei T, Qu L, Zhang M, Yuan L (2019) Method to quantitatively partition the temporal preferential flow and matrix infiltration in forest soil. *Geoderma* 347:150–159. <https://doi.org/10.1016/j.geoderma.2019.03.026>
- Zhao Z, Shen Y, Shan Z, Yang Y, Zhao G (2018) Infiltration patterns and ecological function of outcrop runoff in epikarst areas of Southern China. *Vadose Zone J* 17(1):1–10. <https://doi.org/10.2136/vzj2017.11.0197>
- Zhao ZM, Shen YX, Jiang RH, Wang QH (2020) Rock outcrops change infiltrability and water flow behavior in a karst soil. *Vadose Zone J* 19(1):e20002. <https://doi.org/10.1002/vzj2.20002>

**Publisher's Note** Springer Nature remains neutral with regard to jurisdictional claims in published maps and institutional affiliations.